

HENRY

Hydraulic Engineering Repository

Ein Service der Bundesanstalt für Wasserbau

Conference Paper, Published Version

Nakagawa, Hajime; Satofuka, Yoshifumi; Oishi, Satoru; Muto, Yasunori; Sayama, Takahiro; Takara, Kaoru; Sharma, Raj Hari

Observations and Modeling of Rainfall and Sediment Runoff in the Lesti River Basin, Tributary of the Brantas River, Indonesia

Zur Verfügung gestellt in Kooperation mit/Provided in Cooperation with:
Kuratorium für Forschung im Küsteningenieurwesen (KFKI)

Verfügbar unter/Available at: <https://hdl.handle.net/20.500.11970/110128>

Vorgeschlagene Zitierweise/Suggested citation:

Nakagawa, Hajime; Satofuka, Yoshifumi; Oishi, Satoru; Muto, Yasunori; Sayama, Takahiro; Takara, Kaoru; Sharma, Raj Hari (2008): Observations and Modeling of Rainfall and Sediment Runoff in the Lesti River Basin, Tributary of the Brantas River, Indonesia. In: Wang, Sam S. Y. (Hg.): ICHE 2008. Proceedings of the 8th International Conference on Hydro-Science and Engineering, September 9-12, 2008, Nagoya, Japan. Nagoya: Nagoya Hydraulic Research Institute for River Basin Management.

Standardnutzungsbedingungen/Terms of Use:

Die Dokumente in HENRY stehen unter der Creative Commons Lizenz CC BY 4.0, sofern keine abweichenden Nutzungsbedingungen getroffen wurden. Damit ist sowohl die kommerzielle Nutzung als auch das Teilen, die Weiterbearbeitung und Speicherung erlaubt. Das Verwenden und das Bearbeiten stehen unter der Bedingung der Namensnennung. Im Einzelfall kann eine restriktivere Lizenz gelten; dann gelten abweichend von den obigen Nutzungsbedingungen die in der dort genannten Lizenz gewährten Nutzungsrechte.

Documents in HENRY are made available under the Creative Commons License CC BY 4.0, if no other license is applicable. Under CC BY 4.0 commercial use and sharing, remixing, transforming, and building upon the material of the work is permitted. In some cases a different, more restrictive license may apply; if applicable the terms of the restrictive license will be binding.

OBSERVATIONS AND MODELING OF RAINFALL AND SEDIMENT RUNOFF IN THE LESTI RIVER BASIN, TRIBUTARY OF THE BRANTAS RIVER, INDONESIA

Hajime Nakagawa¹, Yoshifumi Satofuka², Satoru Oishi³, Yasunori Muto⁴,
Takahiro Sayama⁵, Kaoru Takara⁶ and Raj Hari Sharma⁷

¹ Professor, Disaster Prevention Research Institute, Kyoto University
Shimomisu, Yoko-oji, Fushimi-ku, Kyoto 612-8235, Japan, e-mail: nakagawa@uh31.dpri.kyoto-u.ac.jp

² Professor, Department of Civil and Environmental Systems Engineering, Ritsumeikan University
1-1-1, Noji-higashi, Kusatsu-shi, Shiga 525-8577, Japan, e-mail: y_satofuka@yahoo.co.jp

³ Associate Professor, Interdisciplinary Graduate School of Medicine and Engineering, University of Yamanashi
4-3-11, Takeda, Kofu-shi, Yamanashi 400-8511, Japan, e-mail: tetsu@yamanashi.ac.jp

⁴ Associate Professor, Disaster Prevention Research Institute, Kyoto University
Hatazaki Katata, Shirahama, Wakayama 649-2201, Japan, e-mail: muto_yas@mbox.kudpc.kyoto-u.ac.jp

⁵ Assistant Professor, Disaster Prevention Research Institute, Kyoto University
Gokasho, Uji, Kyoto 611-0011, Japan, e-mail: sayama@flood.dpri.kyoto-u.ac.jp

⁶ Professor, Disaster Prevention Research Institute, Kyoto University
Gokasho, Uji, Kyoto 611-0011, Japan, e-mail: takara@flood.dpri.kyoto-u.ac.jp

⁷ Post Doctoral Fellow, Institut für Geotechnik, TU Bergakademie Freiberg
Gustav-Zeuner-Straße 1, Freiberg 09596, Germany, e-mail: rajharisharma@yahoo.com

ABSTRACT

Intensive and continuous observations on sediment yield and transport are conducted in the Lesti River Basin, a tributary of the Brantas River, Indonesia. This paper presents the observation results of raindrop characteristics investigated with Micro Rain Radar (MRR), seasonal and inter-annual land cover change detected by remotely sensing, soil erosion measurements with staves installed at different land covers, river discharge and velocity measurements with Acoustic Doppler Current Profiler (ADCP), and sediment turbidity measurements at the outlet of the Lesti River. By referring these observation data, we newly developed two models which can reproduce observed rainfall and sediment runoff processes by introducing the NDVI (Normalized Difference Vegetation Index) values that can express land cover changes. Calculated water discharges and turbidity by using each model agree fairly well with observed data.

Keywords: rainfall and sediment runoff, vegetation index, Brantas River, modelling

1. INTRODUCTION

Integrated sediment management is crucial for water resources and river environment, especially when dam reservoirs are located at downstream of erodible volcanic area, such as the upper Brantas River Basin, East Java, Indonesia. The large amount of sediment yielded in the basin brings severe sedimentation problems affecting reservoir capacity. Intensive erosion control is necessary with the understanding of dominant sediment sources and their trends based on the seasonal and inter-annual variability of land cover conditions.

Our study area, the Lesti River Basin (625 km²), is located at the upstream of the Brantas River Basin (11,800 km²) (see Figure 1). The Lesti River Basin is mostly covered with volcanic soil originated from Mt. Semeru, an active volcano located at the upstream of the Lesti River. At the confluence of the Lesti River and the Brantas main reach, Sengguruh

dam was constructed in 1988 for water resources and power generation. Unexpectedly, most of the gross storage (21.5 million m³) has been already filled with sediment from both rivers.

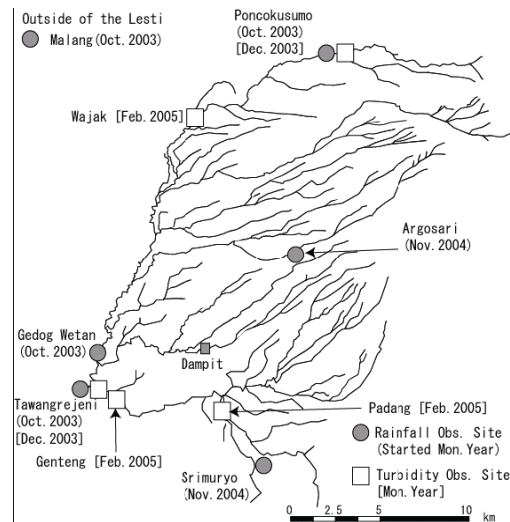


Figure 1 Map of the Lesti River Basin and observation sites.

In the tropical volcanic region, considerable sediment may be yielded by soil erosion, especially during severe storms in a rainy season. Investigations of rainfall characteristic including raindrop distribution size and the impact energy of rain drops are effective to understand the mechanism of soil splash erosion. For this purpose, we newly arranged several rain gauges (see Figure 1) and used a Micro Rain Radar (MRR) to observe rainfall characteristics in the upper Brantas River Basin. The land cover condition has also significant impact on the sediment erosion. Multi-temporal remotely sensed data are used to clarify the seasonal and inter-annual land cover change in a catchment scale. We carried out also continuous soil erosion observations with staves installed at different land use regions. In addition to these soil erosion observations, we conducted field measurements of discharge and turbidity from the outlet of the Lesti River. We used Acoustic Doppler Current Profiler (ADCP) to measure the profile of velocity and discharge in a river channel. The results confirmed the accuracy of operational continuous discharge measurements based on H-Q relationship. Continuous turbidity measurements as well as intensive turbidity observations are also carried out to estimate sediment load from the outlet (Nakagawa, et al., 2005).

2. DATA OBSERVED

Rainfall Characteristics with a MRR

In this research, the one dimensional Doppler radar, Micro Rain Radar (hereinafter, called MRR) and the tipping bucket rain gage is used in Malang city, Indonesia. The observation period started from December 22, 2003 to March 23, 2004. MRR is a one dimensional dopplar radar that release the microwave of 24 GHz. The MRR is set on the top of the roof of JASA TIRTA I public corporation in Malang city, Indonesia. The dopplar spectrum which has information of falling speed of rain drops is measured as well as the radar echo which has information of amount of rain drops. Therefore, rain drop size distribution from diameter of 0.21 mm to 4.08 mm is estimated by MRR. In this research, the size distribution of 0 m to 200 m above the ground is used. Rain drop energy per unit area per unit time E [W/m²] is expressed as follows:

$$E = \frac{\pi}{12} \rho_w \int_0^{\infty} N(D) D^3 v^3(D) dD \quad (1)$$

where, D : diameter of rain drop [mm], $N(D)$: rain drop size distribution function [$1/m^3 / mm$], $v(D)$: falling speed of rain drop of diameter D .

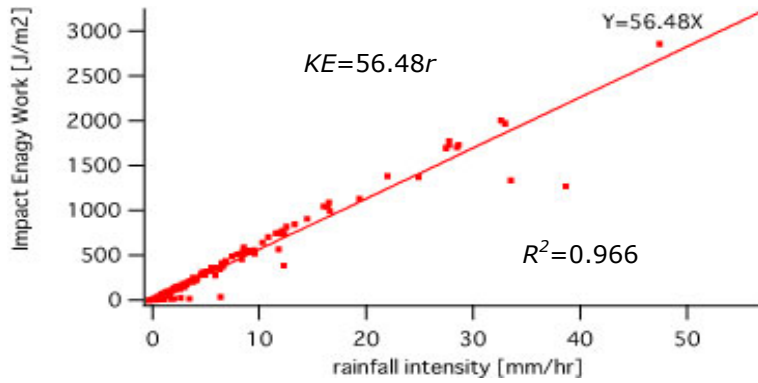


Figure 2 Relationship between impact work of one hour and rainfall intensity.

Figure 2 shows the scattergram of rainfall intensity versus impact work of one hour. The figure shows that there is very strong linear correlation between them and the square of correlation coefficient is 0.966 (Oishi, et al., 2005).

Landcover Classification with Remotely Sensed Data

Land cover condition in the Lesti River Basin is studied using three kinds of remotely sensed data including ADEOS/AVNIR (16 m resolution, July 1997), LANDSAT7/ETM+ (30 m resolution, May 2002), and multiple scenes of TERRA/MODIS NDVI (250 m resolution

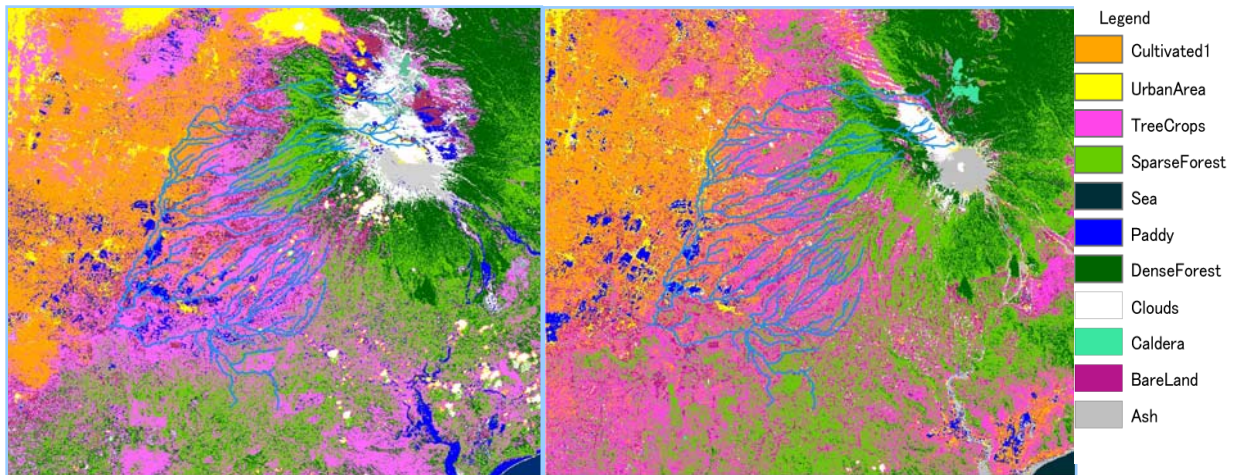


Figure 3 Land cover classification maps based on ADEOS/AVNIR captured in 1997 (left) and LANDSAT7/ETM+ captured in 2002 (right).

16 days composite, from 2002 to 2003). Figure 3 shows two land cover classification maps based on ADEOS/AVNIR and LANDSAT7/ETM+. There is no significant difference between two scenes except for some erroneous area due to cloud cover and some area outside the Lesti River basin. Large-scale landuse change was not found inside the basin from 1997 to 2002. On the other hand, TERRA/MODIS NDVI (see Figure 4) captured in different seasons

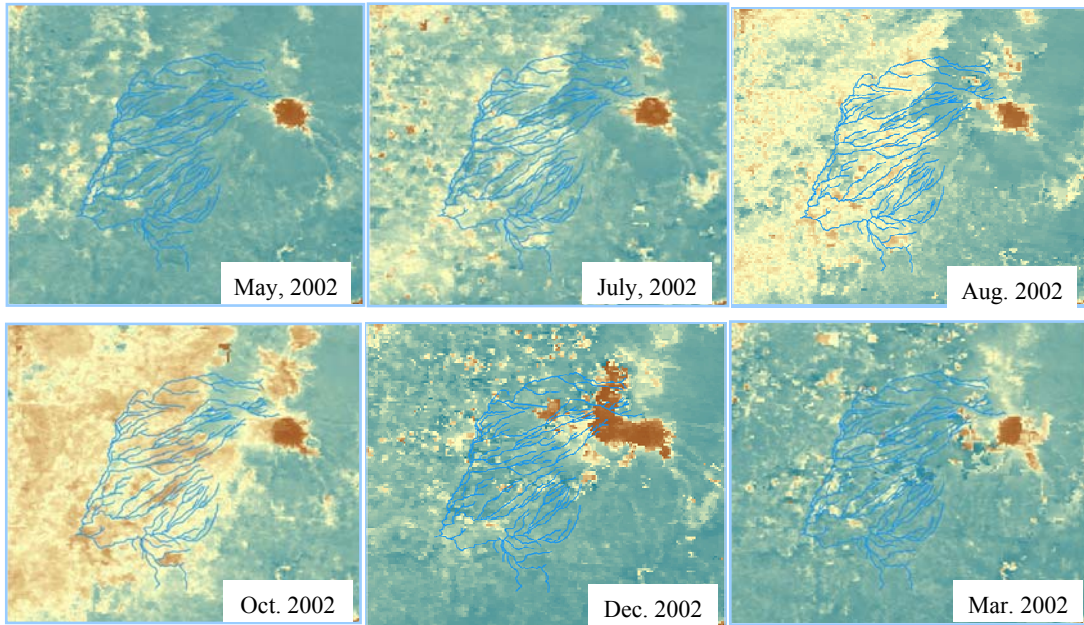


Figure 4 Seasonal Variability of NDVI (Normalized Difference Vegetation Index) (TERRA/MODIS, 250m resolution).

indicate seasonal variability of vegetation cover. Figure 5 shows average NDVI values based on TERRA/MODIS images for each land cover class, which is obtained from LANDSAT7/ETM+. NDVI becomes the lowest in the end of a dry season especially in is obtained from LANDSAT7/ETM+. NDVI becomes the lowest in the end of a dry season especially in cultivated land and in tree crops area, while forest areas maintain relatively high NDVI for all seasons. It is expected that this high seasonal variability of vegetation activity influences on sediment yield processes; especially, the tendency that cultivated and tree crops zone becomes almost bare land in the beginning of a rainy season may activate sediment erosion at the time.

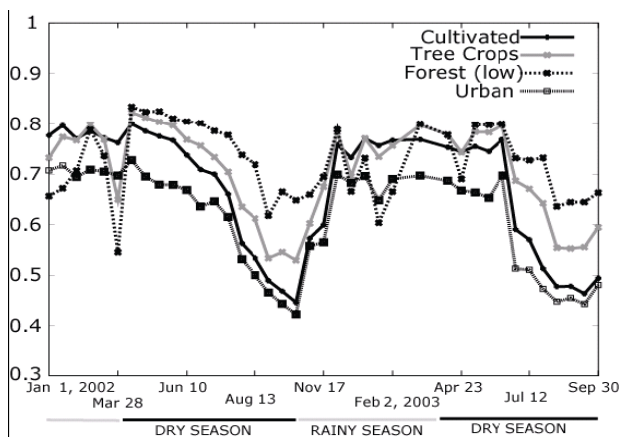


Figure 5 Seasonal trends of NDVI in land cover classes.

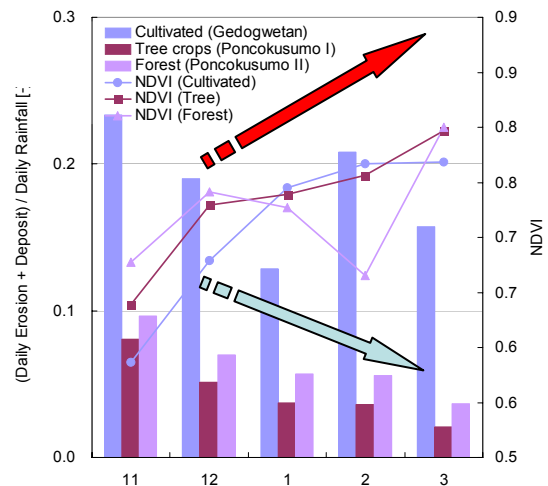


Figure 6 Relationship between soil movement depth per rainfall and NDVI values in the three types of landuse.

Soil Erosion

The analyses of rainfall impact energy discussed in section two indicated the linear relationship between rainfall and soil erosion rate. In order to parameterize the linear relation,

we conducted continuous soil erosion measurement at three types of landuse including cultivated (Gedog Wetan), tree crops (Poncokusumo I) and forest area (Poncokusumo II) (see Figure 1). Four staves are installed at different slope for each landuse area. Then responsible local people kindly measure and take photographs of scales on the staves everyday. The measurement started in October 2003.

Figure 6 shows relationship between soil movement depth (absolute daily depth including erosion and deposit) per rainfall [-] and NDVI values in the three types of landuse. The sediment movement depth shown in Figure 6 is expected to represent the sediment detachment rate parameter. The results confirm around three times higher sediment activity in the cultivated land than the other two landuse areas. In addition, while in the tree crops and forest area the sediment moving rate is decreased as the time passed after November, two peaks of the rate were observed in the cultivated area. It is interesting to discuss the same tendency was observed from the turbidity measurements discussed in next section with some considerations of double cropping in the Brantas River Basin.

Sediment and Water Discharge

In order to estimate the amount of sediment flow into Sengguruh Dam from the Lesti River basin, information on sediment discharge in the Lesti River is necessary. According to preliminary survey, most of sediment in the Lesti River is loaded in a suspended form (mean diameter of the sediment flowing in the channel, $d_m = 30\mu\text{m}$). In addition, sediment distributions in a cross section was checked by a potable turbidity meter (ALEC ATU-30D) under a non-flood condition and was shown to be nearly uniform. Thus point-measured turbidity data at Tawangrejeni (see Figure 1) by JASA TIRTA I can be used as a characteristic value for the whole section. In the followings analyses and discussions are made based on this JASA TIRTA I's data.

Figure 7 shows temporal variation of turbidity at Tawangrejeni, together with variation of discharge in 2003. The unit of the measured turbidity is FNU, which can be translated into ppm by using the following equation:

$$\text{ppm} = 0.0401 \times \text{FNU} + 0.0278 \times (\text{FNU})^2 \quad (2)$$

It seems in the figure that when discharge increases turbidity also becomes large, but at the same time one will notice that there are several points where turbidity is so high but discharge does not increase so much. It can therefore be said that there is no correlation between these two parameters in magnitude. In other words, turbid flow occurs irrespective of the local discharge at Tawangrejeni.

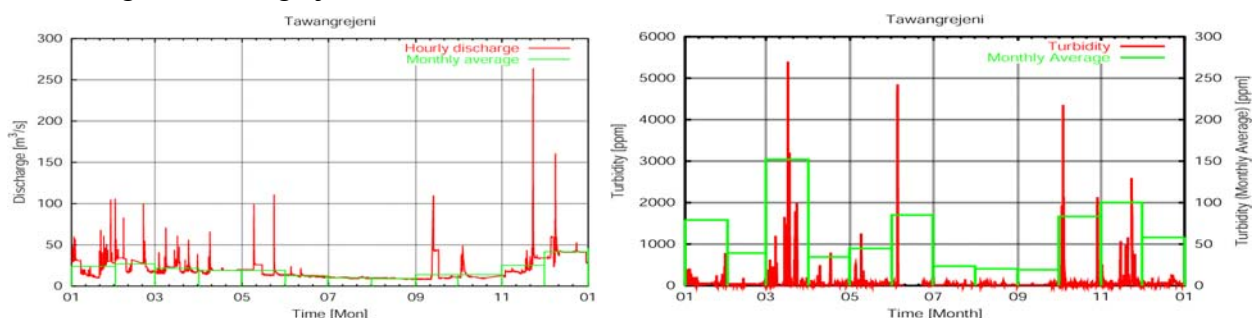


Figure 7 Observed water discharge and turbidity at Tawangrejeni in 2003.

Sediment discharge per unit time can be obtained by multiplying discharge and turbidity. Figure 8 shows the sediment discharge based on the data in Figure 7. The figure clearly shows that there are two peak seasons, early spring and autumn. The rainy season of the catchment area is from October to March. Therefore it is deemed that large sediment

discharges in floods in the rainy season, in which the deposited sediments on the slopes during the dry season are washed away into rivers. The other peaks in early spring could be related to cultivation. Takaya (1985) cited Mahoney report (1982) and describe cultivation in East Java, that they have harvest twice in one rainy season, and the second cultivation usually starts in March. Sediments in early spring could result from soils in cultivation fields, disturbed at the beginning of the second cultivation.

Direct measurements for sediment concentration were also carried out at Wajak, about 14 km upstream from Tawangrejani (see Figure 1), in March 2005. The river discharge was increased just after some rains. Velocity distributions were measured by an electro-magnet current meter, and were integrated to give the river discharge of 6.5 m³/s. Turbid water was sampled by a bottle and was analyzed in a laboratory, then the measured turbidity was 12,600mg/liter. Sediment discharge can be calculated as 295 ton/h, which is the same order as the peak values shown in Figure 7.

3. DISTRIBUTED RAINFALL AND SEDIMENT RUNOFF MODEL

We newly developed two models which can reproduce observed rainfall and sediment runoff processes by introducing the NDVI values that can express land cover changes. Those models, named as ‘‘ST Model’’ and ‘‘RH Model’’, respectively, are both in the kinematic wave runoff models and are rather similar. The important difference in those models comes from treatment of effects of NDVI on the erodibility of the topsoil.

ST Model

We use a distributed rainfall-runoff model that simulates unsaturated, saturated subsurface flow and surface flow (Tachikawa et al., 2004). Figure 8 presents the schematic of the model structure applied to each grid-cell. The following mass balance equation and the momentum equations are used to simulate flow from each grid-cell.

$$\frac{\partial h}{\partial t} + \frac{\partial q}{\partial x} = r(t) = f \cdot R(t) \quad (3)$$

$$q = \begin{cases} v_c d_c (h/d_c)^\beta & , (0 \leq h \leq d_c) \\ v_c d_c + v_a (h - d_c) & , (d_c < h \leq d_s) \\ v_c d_c + v_a (h - d_c) + \alpha (h - d_s)^m & , (d_s < h) \end{cases} \quad (4)$$

where h : water stage, q : discharge per unit width, $r(t)$: effective rainfall, f : runoff coefficient accounting for the water loss by evapotranspiration and canopy interception, $R(t)$: observed rainfall, d_c, d_s : effective depths corresponding to the maximum water depths in the matrix and macro-pore parts. v_c, v_a : average flow velocities of unsaturated subsurface flow and saturated subsurface flow, which are expressed as

$$v_c = k_c i, \quad v_a = k_a i \quad (5)$$

where, k_c, k_a : saturated hydraulic conductivities in the matrix part and the macro-pore part, i : slope gradient. In Eq.2, $\alpha = \sqrt{i}/n$ where n : roughness coefficient, $\beta = k_a/k_c$, m : constant (= 5/3), t : time, and x : distance.

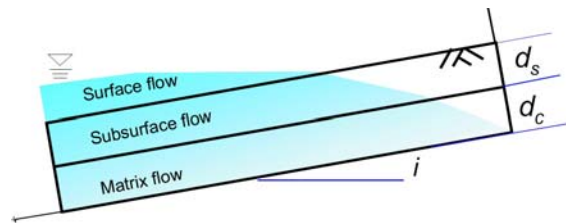


Figure 8 Schematic view of surface and subsurface flow.

For the sediment transportation model incorporated into the distributed rainfall-runoff model, we use the following sediment mass balance equation, in which D_r represents rain drop splash erosion and D_f represents sediment yield by surface flow shear stress (Govers and Rauws, 1986).

$$\frac{\partial(h_s c)}{\partial t} + \frac{\partial(q_s c)}{\partial x} = e(x, t) = D_r + D_f \quad (6)$$

$$D_r = K \cdot K_e, \quad D_f = \delta(c_t - c)h_s \quad (7)$$

where h_s : flow depths of the surface flow, c : sediment concentration, q_s : surface flow discharge per unit width. K : erodibility coefficient ($=0.002\text{kg/J}$), K_e : kinetic energy of the net rainfall, δ : parameter for flow erosion, c_t : sediment transportation capacity.

RH Model

In ‘‘RH Model’’, the basic equations are rather similar but the most significant difference is that in the ‘‘RH Model’’, NDVI is not considered in evaluating the topsoil erosion by the rain drop impact, but is considered in the flow resistance, i.e., Manning’s roughness coefficient. This is because that when NDVI value is large, i.e., vegetation on the land-surface is very active, the flow resistance due to vegetation becomes large. The relationship between NDVI value and Manning’s roughness coefficient is established as (Sharma, 2006):

$$n = 0.0713\exp(2.8p) \quad (8)$$

where, n =Manning’s roughness coefficient ($\text{m}^{-1/3}\text{s}$), and p =NDVI value obtained from the satellite data taken in December 2002. It is of course that Eq.(8) is only available in December.

4. MODEL APPLICABILITY

ST Model

We adopt the K_e value obtained by the observations using MRR shown in Figure 2. It clearly shows the linear relationship between the two variables, which can be quantified as follows:

$$K_e = 56.48r \quad (\text{Unit: J/m}^2) \quad (9)$$

Note that the sediment related terms in the Eqs. 6 and 7 are calculated as follows,

$$e(x, t) = (D_r + D_f) / 3600 \quad (\text{Unit: kg/h/m}^2) \quad (10)$$

$$D_f = \delta(\varepsilon c_t / 1000 - c)h_s \quad (\text{Unit: kg/h/m}^2) \quad (11)$$

$$c_t = 187.4v_s i - 125.4 \quad (\text{Unit: ppm}) \quad (12)$$

where v_s : the average velocity of surface flow, δ , ε : parameters ($= 0.9$ and 0.2 for the present study). Figure 9 shows the simulated and observed discharge and turbidity at Tawangrejeni (a) from October 3 to 7, 2003 and (b) September 19 to 20, 2005. The model can simulate both discharge and turbidity reasonably well.

We incorporate the seasonal variability and the effect of land covers on the soil erodibility into the model. As shown in Figure 10, there is negative correlation between NDVI (obtained from satellite images) and erodibility (measured in the field). In addition the erodibility differs depending on the land cover: the erodibility is higher in cultivated land than in tree cropland or forest. Based on this observed findings, we attempt to model the seasonal

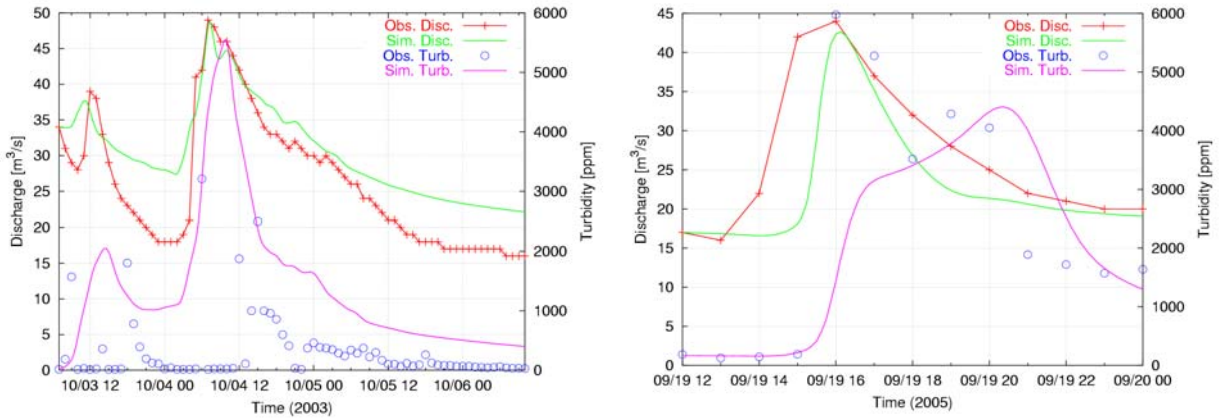


Figure 9 Comparisons between calculated and observed water discharge and turbidity in 2003 flood (a) and in 2005 flood (b). ($\delta = 0.9$, $\varepsilon = 0.2$, $K = 0.2 \times 0.002$)

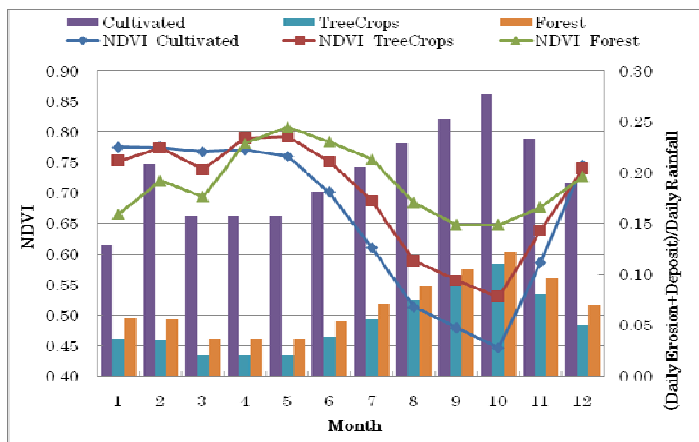


Figure 10 Seasonal change of the erodibility of the top soil (right) and NDVI (left)

effect and the land cover effect by introducing a coefficient μ representing the erodibility (the values shown in Figure. 10). Namely D_r is modified to be $\mu K_l K_e$, where K_l is introduced as a tuning parameter.

Figure 11 shows the long-term simulation results based on the modified model. Although the simulated discharge is sometimes underestimated, the seasonal variability in the observed turbidity is well represented by the model.

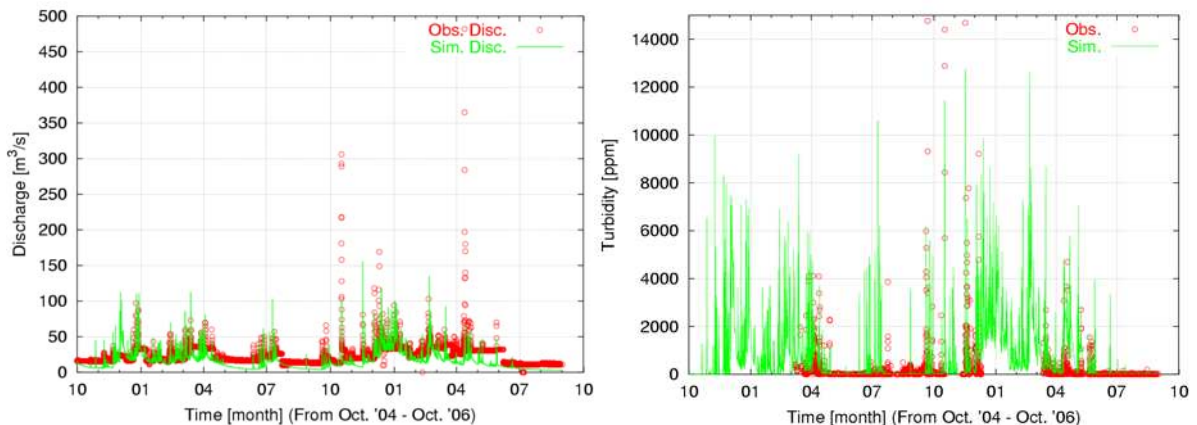


Figure 11 Comparisons between calculated and observed long term water discharges (left) and turbidity (right) at Tawangrejeni from October 2004 to October 2006.

RH Model

Figure 12 shows distribution of roughness coefficient evaluated by using Eq.(8) in the Lesti River basin. NDVI values are obtained from the satellite data taken in December 2002.

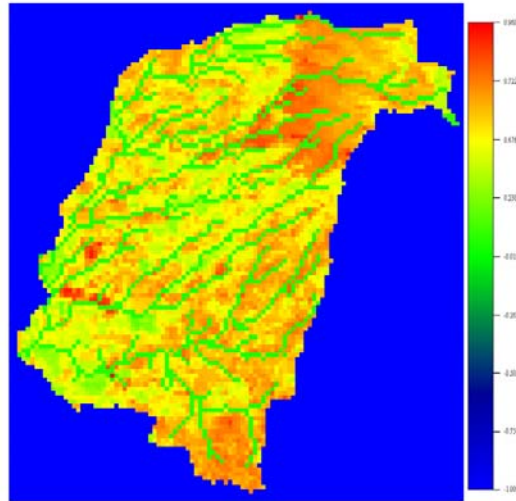


Figure 12 Distribution of evaluated roughness coefficient using Eq.(8) in the Lesti River basin.

Figure 13 shows the comparisons between calculated and observed water discharge (left) and turbidity (right) at Tawangrejeni in the period from 0:00, Nov. 21, 2003 to 0:00, Nov. 24, 2003 by using Eq.(8) as the date is near December. Simulated discharges are in good agreement with the observed one. The simulation in the turbidity is reasonable, considering the simplicity of the model.

5. CONCLUSIONS

Intensive and continuous observations on sediment yield and transport are conducted in the Lesti River Basin, a tributary of the Brantas River, Indonesia. Data obtained were analyzed, and based on these data, distributed rainfall and sediment runoff modes were developed. Followings are summarized results obtained:

- (1) We carried out the various analyses of data obtained by field observations and remote sensing to understand the basin-wide rainfall and sediment runoff processes.
- (2) Sediment yield was found to happens due to heavy rainfall just beginning of the rainy season in the volcanic river basin such as the Lesti River basin.
- (3) At the beginning of rainy season, as the vegetation activity is low yet, a lot of sediment were easily yielded by the raindrop shower, resulting in the high turbidity in the river.
- (4) The distributed rainfall and sediment runoff models, that are based on the erodibility variation due to landuse change, seasonal change of the vegetation, and raindrop impacts, were developed and long- and short-term predictions of sediment runoff phenomenon could be reproduced fairly well.

As expected effects in future, followings can be pointed:

- (5) Highly accurate prediction for the inflow sediment volume into reservoirs may be possible.
- (6) Highly accurate prediction for the amount of sediment volume by erosion corresponding to the surface cover condition (human impact) with vegetation by using NDVI values from satellite image can be possible.
- (7) Suggestions to the farmers for the deliberate land use and development of agronomical

technologies can be possible.

ACKNOWLEDGMENTS

This study was supported by “System Modeling Approaches for Assessment of Interaction between Social Changes and Water Cycle (PI: Prof. Kaoru Takara, DPRI, Kyoto Univ.)”, which was conducted under CREST (Core Research for Environmental Science and Technology) Program by the Japan Science and Technology Agency. JASA TIRTA I Corporation kindly provided some of the presented data and supported our field observations.

REFERENCES

- Govers, G. and Rauws, G. (1986), Transporting capacity of overland flow on plane and on irregular beds, in *Earth Surface Processes and Landforms*, 11, pp.515-524.
- Nakagawa, H., Satofuka, Y., Muto, Y., Ohishi, S., Sayama, T. and Takara, K. (2005), On sediment yield and transport in the Lesti River basin, a tributary of the Brantas River, Indonesia, -Experiences from field observations and remotely sensed data-, in *Proc. of the International Symposium on Fluvial and Coastal Disasters*, CD-ROM.
- Oishi, S, Sayama, T., Nakagawa, H., Satofuka, Y., Muto, Y., Dian Sisinggih and Sunada, K. (2005), Development of estimation method for impact energy of raindrop considering raindrop size distribution and the relationship between the impact energy and local sediment yield, in *Annual Journal of Hydraulic Engineering, JSCE*, 49, pp.1087-1092 (in Japanese).
- Sharma R.H. (2006), Study on integrated modelling of rainfall induced sediment hazards, in *Doctoral thesis of Kyoto University*, pp.71-96.
- Tachikawa, Y., Nagatani, G. and Takara, K. (2004), Development of stage-discharge relationship equation incorporating saturated-unsaturated flow mechanism, in *Annual Journal of Hydraulic Engineering, JSCE*, 48, pp.7-12 (in Japanese).
- Takaya, K. (1985), Nature and land use in South-East Asia, *Tokyo: Keiso-Shobou*, pp.166-177 (in Japanese).

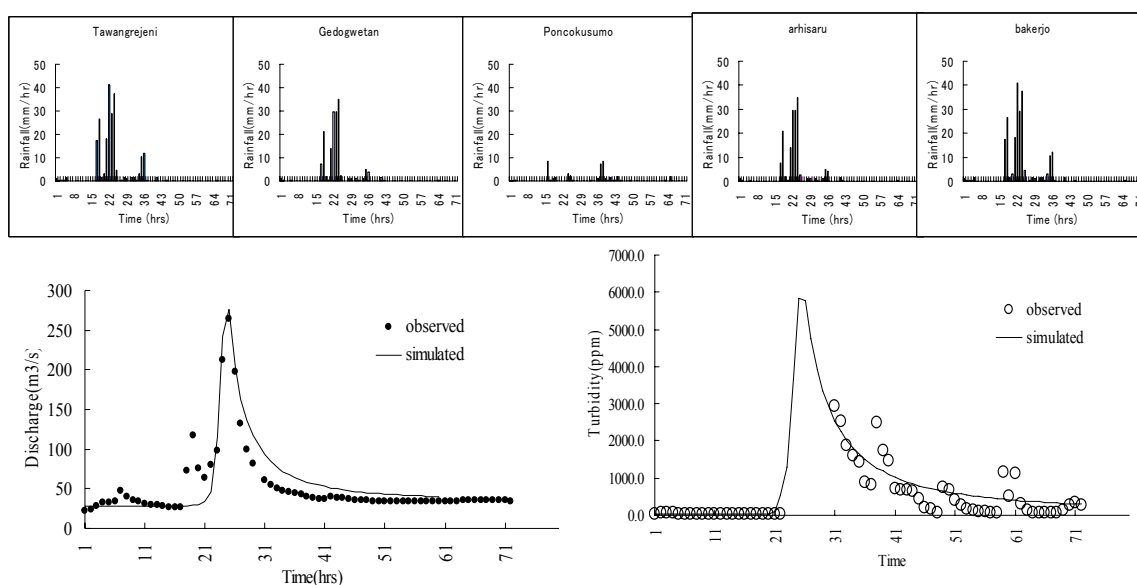


Figure 13 Comparisons between calculated and observed water discharge (left) and turbidity (right) at Tawangrejeni in the period from 0:00, Nov. 21, 2003 to 0:00, Nov. 24, 2003.